

Semantic-aware Binary Code Representation with BERT

Hyungjoon Koo[†] Soyeon Park[‡] Daejin Choi^{*} Taesoo Kim[‡]

Sungkyunkwan University[†], Georgia Institute of Technology[‡], Incheon National University^{}*

ABSTRACT

A wide range of binary analysis applications, such as bug discovery, malware analysis and code clone detection, require recovery of contextual meanings on a binary code. Recently, binary analysis techniques based on machine learning have been proposed to automatically reconstruct the code representation of a binary instead of manually crafting specifics of the analysis algorithm. However, the existing approaches utilizing machine learning are still specialized to solve one domain of problems, rendering recreation of models for different types of binary analysis.

In this paper, we propose DEEPSemantic utilizing BERT in producing the semantic-aware code representation of a binary code. To this end, we introduce *well-balanced instruction normalization* that holds rich information for each of instructions yet minimizing an out-of-vocabulary (OOV) problem. DEEPSemantic has been carefully designed based on our study with large swaths of binaries. Besides, DEEPSemantic leverages the essence of the BERT architecture into *re-purposing* a pre-trained generic model that is readily available as a one-time processing, followed by quickly applying specific downstream tasks with a fine-tuning process. We demonstrate DEEPSemantic with two downstream tasks, namely, binary similarity comparison and compiler provenance (*i.e.*, compiler and optimization level) prediction. Our experimental results show that the binary similarity model outperforms two state-of-the-art binary similarity tools, DeepBinDiff and SAFE, 49.84% and 15.83% on average, respectively.

1 INTRODUCTION

In a modern computing environment, it is not uncommon to encounter binary-only software: *e.g.*, commodity or proprietary programs, system software like firmware and device drivers, etc. Accordingly, binary analysis plays a pivotal role in implementing a wide range of popular use cases [17, 19, 27, 74]: *e.g.*, code clone or software plagiarism detection to protect against intellectual property infringement [23, 46, 77], vulnerability discovery on distributed software [13, 14, 20, 21, 25, 44, 48, 57, 58, 63, 65], malware detection [11, 12, 41] and classification [34, 40], program repair or patch analysis [26, 35, 73], and toolchain provenance [54, 62] for the digital forensics purpose.

However, analyzing a binary code is fundamentally more challenging than the source code-based analysis because it has to infer underlying contextual meanings from the machine-interpretable binary code alone. Unlike the representation of human-readable source code, a binary code is a final product out of a complicated compilation process that involves massive transformations (*e.g.*, optimizations), such as control flow graph alteration, function inlining, instruction replacement and dead code elimination, which eventually discards a majority of high-level semantic information

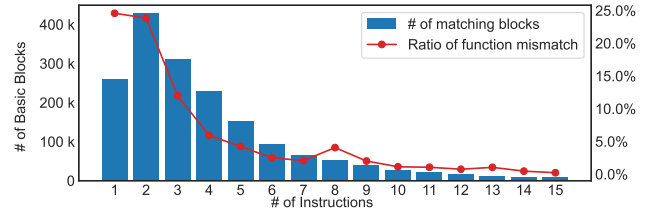


Figure 1: Histogram for the number of matching block pairs (left label) and the ratio of function mismatch (right label) by the number of instructions per basic block with DeepBinDiff [77] from our evaluation dataset (§6). The function mismatch represents basic block pairs with a sequence of identical instructions that do not belong to the same function. More than eight out of 10 from the whole matching basic blocks incorporate 5 instructions or less.

useful for analysis. Besides, there are other major factors that impact code generation, such as an architecture, compiler, compiler version or option and code obfuscation.

Recently, machine learning-based techniques [13, 17, 19, 23, 27, 42, 44, 49, 74, 76–78, 83] have been proposed as a promising direction to address this code semantic problem in binaries. Although traditional approaches like static analysis (*e.g.*, graph isomorphism on call graph [21, 25]) or dynamic analysis (*e.g.*, taint analysis [24, 57]) have shown a high accuracy in specific tasks, machine learning-based approaches are often much favorable in rapidly changing computing environments: as far as training data is provided, one model can be reused for multiple platforms and architectures, as well as it can be constantly improved with the increasing number of new inputs. Indeed, the recent state-of-the-art tools [23, 49, 77, 78, 83] successfully generate code embedding (vector) for semantic clone detection across architecture [78, 83], optimization [23, 49, 77], and even obfuscation [23].

However, we question both the means and quality of code embedding to infer code semantics in terms of applicability in practice. For instance, Figure 1 illustrates the matching basic block pairs and function mismatch cases with our DeepBinDiff [77] evaluation dataset (§6). According to our experiment, 83% of the whole matching block pairs consist of 5 instructions or less. Besides, we examine function mismatch cases (*i.e.*, matching block pairs that consist of identical instructions, which belong to different functions): 14.1% of such block pairs contain five instructions or less whereas 1.5% contain six or more, which implies that a block granularity for a binary similarity task is often insufficient to deduce code semantics. In particular, most basic block pairs with one or two instructions consist of `nop`, `jmp` or `call`.

In this regard, we investigate large swaths of binary code that include approximately 108 million machine instructions or 1.7 million binary functions, summarizing our insights as follow. First, the distribution of the instructions follows Zipf’s law [82] analogous to a natural language. Second, oftentimes a function conveys contextually meaningful information. Third, word2vec [50] lacks diverse representations for the identical instruction in a different position. Fourth, graph information (e.g., control flow graph) may not play a pivotal role to determine code semantics, which aligns with the recent findings [48].

To this end, we present DEEPSemantic, an architecture that is capable of deeply inferring underlying code semantics based on the cutting-edge BERT (Bi-directional Encoder Representations from Transformers) architecture [22]. Based on the above insights, DEEPSemantic has been carefully designed so that it can leverage BERT to achieve our goals including i) *function-level granularity*; e.g., the unit of an embedding is a binary function, ii) *function embedding as a whole*; e.g., each instruction may have multiple representations depending on the location of a function, iii) *well-balanced instruction normalization* that strikes a balance between too-coarse-grained and too-fine-grained normalization, and iv) a *two-phase training model* to support a wide range of other downstream tasks based on a pre-trained model. DEEPSemantic mainly consists of two separate training stages: It creates a one-time *generic code representation* (i.e., pre-trained model or DS-PRE) applicable to any downstream task that requires the inference of code semantics at a pre-training stage, followed by generating a *special-purpose code representation* (i.e., fine-tuned model or DS-TASK) for a given specific task based on the pre-trained model at a fine-tuning stage. Like the original BERT, the former stage employs a general dataset with unsupervised learning, whereas the latter stage makes use of a task-oriented dataset with supervised learning. The key advantage of adopting the two-stage model in DEEPSemantic is to support potential applications that allow for *re-purposing* a pre-trained model to quickly apply other downstream tasks using less expensive computational resources.

We have applied DEEPSemantic to both binary similarity comparison (DS-BINsim) and toolchain provenance prediction (DS-TOOLCHAIN) tasks. The empirical results show that DS-BINsim by far outperforms two state-of-the-art binary similarity comparison tools, obtaining a 49.8% higher F1 than DeepBinDiff [77] (up to 69%) and 15.8% than SAFE [49] (up to 28%) on average. For DS-TOOLCHAIN, we obtain an F1 of 0.96 and 0.91 for compiler and optimization level (compilation provenance) prediction, respectively. In summary, we make the following contributions:

- To the best of our knowledge, our work is the first study to investigate binaries on a large scale to *choose appropriate design* for inferring code semantics.
- We devise *well-balanced instruction normalization* that can preserve as much contextual information as possible while maintaining efficient computation.
- We implement a simplified BERT architecture atop our observations and insights on binaries, which can generate semantic-aware code representations.
- We experimentally demonstrate both the effectiveness and efficiency of DEEPSemantic with binary similarity (DS-BINsim) and

compiler provenance prediction (DS-TOOLCHAIN). In particular, DS-BINsim surpasses the two state-of-the-art binary similarity tools (i.e., DeepBinDiff [77] and SAFE [49]).

The source code of DEEPSemantic will be publicly available including our pre-trained model to foster further binary research in the near future.

2 BACKGROUND

This section describes how we leverage a handful of cutting-edge concepts in the literature of natural language processing (NLP) into building DEEPSemantic.

Binary Code Representation. Binary code represents machine instructions with two digits (i.e., 0 and 1) as the final product after an extremely complicated compilation process. As a binary code holds a very concise representation in that a majority of high-level concepts (e.g., variable name, structure, type, class hierarchy) have been lost due to a wide range of transformations at compilation, it is quite challenging to deduce underlying contextual meanings.

Recurrent Neural Network. A recurrent neural network (RNN) is a specialized type of neural network designed to process sequential data (e.g., text, audio, video and even *code*). The RNN has shown great performance [39] on a sequence prediction task with in-network memory that stores fruitful information (e.g., state changes). However, a naïve RNN struggles with capturing useful information from long sequences because of the vanishing gradient problem [70]. A gating model, such as LSTM (Long Short-Term Memory) [33] and GRU (Gated Recurrent Unit) [16], has been proposed to mitigate such a short memory issue by devising a special cell for long-range error propagation. However, there are still several downsides: i) limited capability of tracking long-term dependencies; simply put, a single vector from an encoder that implies all previous words may lose partial information, and ii) prohibiting parallelizable computation due to sequentiality. A binary function often consists of a number of instructions, necessitating a better architecture than either a strawman RNN or its variants.

Attention and Transformer. The main idea of the Attention [9] mechanism is to consider all input words (at each time step) when predicting an output word, particularly paying attention to a specific word that is associated with the output word for prediction. This helps to capture a contextual relationship between words in a sentence without worrying about a gradient vanishing problem, which is now widely used in a machine translation domain. Transformer [66] proposes a *multi-head self-attention* technique for highly inferring the context of a sentence (a binary function for our purpose) atop the Attention’s encoder-decoder architecture. Self-attention focuses on the inner relationship between input words, and multi-head conceptually considers multiple Attention vectors (e.g., multiple words with positional information to predict the next word). Figure 2 (b) illustrates a single encoder layer: i) taking input vectors from the previous layer for computing an Attention matrix, ii) feeding the resulting vectors into a feed forward neural network (FFNN) in turn, iii) applying both a batch (e.g., across training examples) and layer (e.g., across feature dimensions) normalization between the self-attention and FFNN layers. The original Transformer [66] has six encoders (i.e., six layers as shown in Figure 2 (a)) and six decoders.

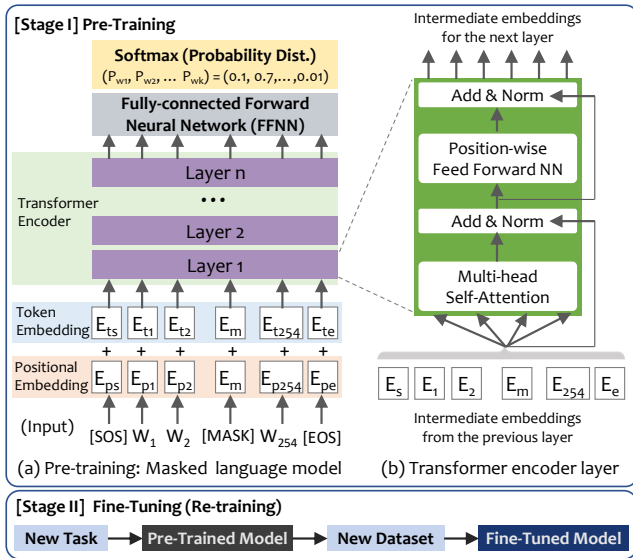


Figure 2: The simplified BERT structure. The key aspects of BERT are i) taking a pre-training stage that generates a generic model and then reuses the model at a fine-tuning stage to create a specific model tailored to a downstream task, and ii) adopting the Transformer’s encoder alone. E denotes an embedding per word W , and the subscripts p , t , m , s , e , and a number represent a position, token, [MASK], [SOS], [EOS], and a word identifier, respectively.

Language Model and BERT. BERT [22], Bi-directional Encoder Representations from Transformers, is one of the state-of-the-art architectures to provide the rich vector representation of a natural language by capturing the contextual meanings of words and sentences (instructions and functions for our model) by adopting the encoder layer of Transformer [66]. It encompasses a number of advanced concepts such as ELMo [56], semi-supervised sequence learning [18] and Transformer. BERT consists of two training phases as in Figure 2: a *pre-training* process builds a generic model with a large amount of corpus and a *fine-tuning* process updates the pre-trained model that is applicable to a specific downstream task. The former takes two strategies: masked language model (MLM) and next sentence prediction (NSP) for building a language model that considers context and the orders of words and sentences, which can be achieved by unsupervised learning with an unlabeled dataset. In Figure 2 (a), the [MASK] token represents an input word that has been masked, and [SOS] and [EOS] are tokens for the start and end of a sentence, respectively ¹. The [UNK] token is used for unknown words. This example has a 256 fixed-length input (254 words with masked ones excluding two special tokens: start/end of a sentence at both ends) at a time. Once the pre-training is complete, the pre-trained model can be recycled for varying user-defined downstream tasks with supervised learning. We adopt BERT because the structure can fit into our objective seamlessly: creating a pre-trained

¹ [CLS] and [SEP] tokens in the original BERT correspond to our [SOS] and [EOS].

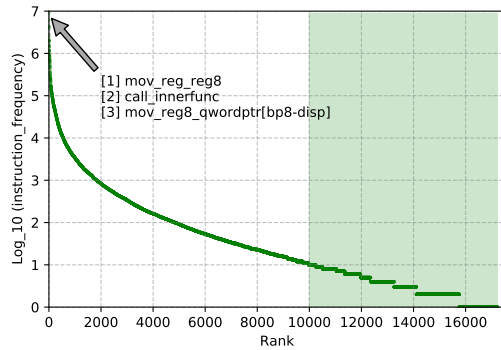


Figure 3: Log scale of instruction frequencies based on each rank in our vocabulary corpus. The curve closely follows Zipf’s law, akin to a natural language. The green area illustrates a long tail that has been rarely seen (e.g., less than 10 times). Interested readers refer to Table 10 in Appendix.

model that contains a generic binary code representation, and re-training that model for a wide range of different classification tasks with relatively lower computational resources (See §4.3 in detail).

3 BINARY CODE SEMANTICS

In this section, we discuss the definition of code semantics, followed by highlighting a few insights of binary codes with common compilation toolchains and optimizations.

3.1 Definition of Code Semantics

We view code semantics in a binary representation differently from the ones in source code. Specifically, the *equivalent semantics of a binary code* can be defined as a sequence of instructions that carries out an identical task from a logical function in the original source. A binary function differs from a programmer-written function due to varying transformations by a compiler toolchain. We use a cosine similarity score ([-1,1] range) that represents the relationship between the two binary functions, meaning that the higher value, the closer in code semantics.

3.2 Observations and Insights

A binary code is a sequence of machine instructions analogous to a natural language. Indeed, InnerEye [83] borrows the ideas of Neural Machine Translation (NMT) to a binary function similarity comparison task by regarding instructions as words and basic blocks as sentences. For successful binary code representation with deep neural networks, it is essential to carefully understand its properties. Here are several insights based on our observation of machine instructions.

- **Machine instructions follow Zipf’s Law.** Figure 3 depicts the relationship between the rank of instructions and the log scale of their frequencies. Our finding shows that the curve of the instruction distribution closely follows Zipf’s law [82] like a natural language, which implies that utilizing effective techniques in an NLP domain such as BERT works for a binary task.

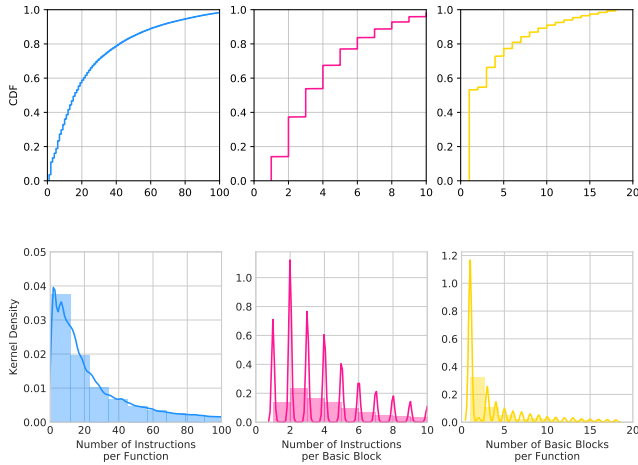


Figure 4: CDFs and histograms with kernel density estimates (10 bins) for the number of instructions per function (left) and basic block (middle), and the number of basic blocks per function (right) after removing outliers. A majority of basic blocks (around 80%) contain merely five instructions or less, indicating that a larger granularity is needed to imply contextually fruitful information.

- **A function often conveys a meaningful context.** We analyze 1,681,467 functions (18,751,933 basic blocks or 108,466,150 instructions) excluding linker-inserted ones in our corpus (Table 3). We measure several statistics: i) the number of instructions per function on average (I/F) is 64.5 (median=19, std=374.7), ii) the number of basic blocks per function on average (B/F) is 5.8 (median=4, std=16.4), and iii) the number of instructions per basic block on average (I/B) is 11.2 (median=3, std=95.8). As the standard deviation is quite large, we remove outliers by cutting off the values that are bigger than the standard deviation times three, which is around 12%, finally obtaining a mean of (I/F, B/F, I/B) = (25.1, 3.9, 3.7). Figure 4 illustrates CDFs (upper) and histograms (below) without outliers, counterintuitively showing that approximately 70% of basic blocks include five instructions or less where a binary function contains around four basic blocks with 25 instructions on average. We choose a granularity as a single function that is large enough to be able to convey contextually meaningful information. Indeed, quite a few matching blocks from our experimental results (Figure 1) using DeepBinDiff [77] contain a couple of instructions (e.g., jmp, call), which are highly likely to miss surrounding contexts². We discuss other cases that a fine-grained granularity becomes beneficial (See §7).
- **Word2vec lacks diverse representations for the same instructions in a different position.** A majority of prior works [23, 77, 83] adopt a Word2vec [50] algorithm to represent a binary code. Word2vec is an embedding technique that aims to learn word relationships from a large corpus text, representing each distinct word with a vector. Figure 5 illustrates the Top 30 most common instructions that are well associated with each

²Instead, DeepBinDiff considers CFGs to read underlying context.

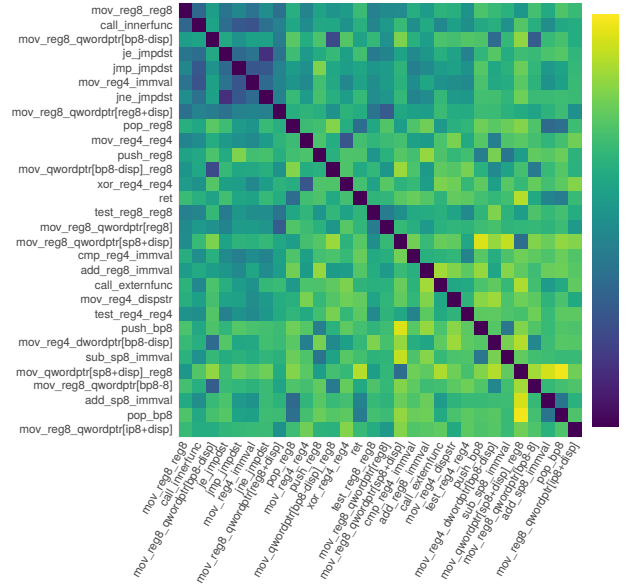


Figure 5: Visualization of a similarity matrix for the most common 30 instructions with a Word2Vec model. The dark color represents that the relationships of two instructions are close to each other. For example, oftentimes ret (middle-left) comes with a series of function epilogue instructions (e.g., pop bp8 and add sp8 immval at the right-bottom corner).

other. Word2vec itself cannot differently represent the identical instruction in a distinct context due to the absence of position information. For instance, a behavior of popping a register for a function epilogue differs from the one for other computation in the middle of the function. However, Word2vec represents the identical representation (embedding) for the same word regardless of their contextual differences, necessitating a better embedding means with the *restricted* number of vocabularies.

- **CFG within a function may not be fruitful.** Previous works often employ a control flow graph [76, 77] ($G(V, E)$; basic block as a vertex and flow as an edge) or graph isomorphism [25] as a feature to compare a binary code. However, our finding shows that both the numbers of vertices and edges do not often stay identical ($|V| \neq |V'|$, $|E| \neq |E'|$) across different optimization levels, to which the isomorphism cannot be applicable. The empirical results of a recent study [48] align with our insight. Instead of having CFGs, we feed such fruitful flow information with well-balanced normalization (§4.2) to deep neural networks (e.g., by defining new words for calling libc functions).

Unlike a natural language, the number of possible instructions is countless when mapping each instruction into a single word (token or vocabulary); an immediate value in a 64-bit operand of the instruction may produce 2^{64} different words, prohibiting further computation. In this regard, most of prior approaches that harness deep learning techniques [23, 77, 78, 83] adopt *normalization* before

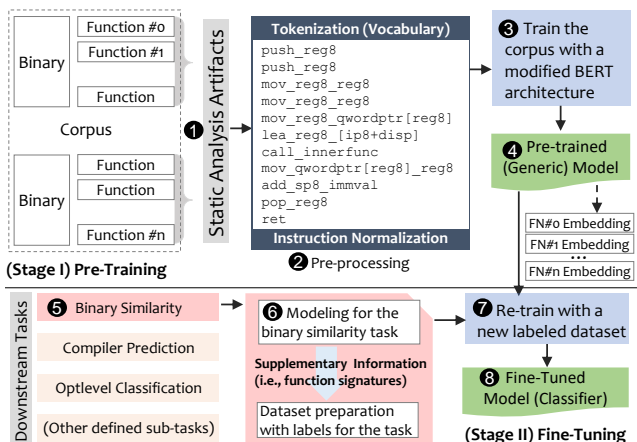


Figure 6: DEEPSemantic Overview. We collect artifacts via static analysis with a pre-defined binary corpus [1]. A pre-processing step tokenizes all instructions with normalization [2] (§4.2). The entire corpus is pre-trained with BERT [3], generating a pre-trained model [4] (§4.3). We define a downstream task (e.g., binary similarity comparison) [5], and prepare another dataset with labels accordingly [6]. Lastly, a fine-tuned model is obtained [8] (§4.4) after re-training the dataset for the task [7].

feeding a sequence of instructions as an input into a training process. In particular, striking a balance is crucial so that instruction normalization is neither too generic nor too specific because each token holds rich information yet minimizing an OOV problem, necessitating a better instruction normalization technique to capture code semantics for neural networks. §4.1 justifies the decision of DEEPSemantic design to comply with our insights.

4 DEEPSemantic DESIGN

In this section, we provide an outline of DEEPSemantic, and portray the design of DEEPSemantic in detail.

4.1 DEEPSemantic Overview

DEEPSemantic consists of two separate stages, as illustrated in Figure 6: i) a pre-training stage that creates a general model applicable to a downstream task, and ii) a fine-tuning stage that generates another model for a specific task on top of the pre-trained model. The following describes four design decisions and their rationales behind DEEPSemantic:

- **Function-level Granularity.** We determine a function as a minimum unit that can imply meaningful semantics from our insights in §3.2. Indeed, our experiment shows a large portion (e.g., 83.25%) of basic block matching results from previous results [77] come from very small basic blocks as in Figure 1.
- **Function Embedding.** Along with the function-level granularity, DEEPSemantic generates an embedding per function as a whole, rather than per instruction (e.g., word2vec) for code representation. This means even an identical instruction would

have a different embedding upon its position and surrounding instructions (Figure 2).

- **Well-balanced Normalization.** We leverage the existing static binary analysis to normalize instructions so that a pre-training model can naturally embrace important features in a deep neural network. We intentionally attempt to remain as much information (manually engineered features from previous studies [24]) as possible (§4.2).
- **Model Separation.** Unlike prior approaches, our model requires two trainings: one for pre-training and another for fine-tuning per user-defined task. The flexible design of DEEPSemantic suits a wide range of domain-specific sub-tasks, which we will showcase two applications: a binary similarity and toolchain prediction (§4.4) task.

As DEEPSemantic inherently generates multiple models, the pre-training and fine-tuning models are dubbed DS-PRE and DS-TASK, respectively, depending on the task (e.g., DS-BINSIM for binary similarity, DS-TOOLCHAIN for compiler provenance).

4.2 Well-balanced Normalization

An instruction normalization process is essential to prepare its vectorization form fed into a neural network as adopted by many prior approaches [23, 49, 77, 78, 83]. However, a too coarse-grained normalization, such as stripping all immediate values [23, 77, 83] loses a considerable amount of contextual information whereas a too fine-grained normalization close to instruction disassembly raises an OOV problem due to a massive number of unseen instructions (tokens). We observe that the previous approaches solely perform mechanical conversion of either an opcode or operand(s) without thorough consideration on their contextual meanings. Figure 7 shows different normalization strategies taken by several approaches for binary similarity detection. DeepBinDiff [77] considers a register size to symbolize an n-byte register (8); however, it converts all immediates into `imme` (9). Meanwhile, InnerEye [83] discards the size information of registers (10) for a 64-bit machine instruction set. SAFE [49] retains immediate values (7). Besides, all three cases convert the destination of a call invocation into a single notation (e.g., `HIMM`, `imme`, or `F00`), rendering every call instruction identical.

To this end, we establish a *well-balanced normalization strategy* to strike a balance between expressing binary code semantics as precisely as possible and maintaining reasonable amount of tokens, that is, a small number of tokens may lose original semantics whereas a large number of tokens may suffer from an OOV problem. The quality of instruction normalization is of significance because word embeddings eventually rely on an individual normalized instruction, holding final contextual information. For instance, an immediate can imply one of the following: a target of library, call invocation within or out of the current binary, destination to jump to, string reference, or statically-allocated variable; however dropping such an implication makes the embedding rarely distinguishable from each other. For instance, the two most frequent words (`mov_reg8_ptr` and `mov_reg8_reg8`) out of two thousand vocabularies when applying coarse-grained normalization account for more than 20% of appearances, according to our experiment, which

| Original Disassembly | DeepSemantic | SAFE | DeepBinDiff | InnerEye |
|----------------------------------------------------------------------------------------------------------------------------------------------------------------------------------------------------------------------------------|----------------------------------------------------------------------------------------------------------------------------------------------------------------------------------------------------------------------------|---------------------------------------------------------------------------------------------------------------------------------------------------------------------------------------------------------------------|-------------------------------------------------------------------------------------------------------------------------------------------------------------------------------------------------|-------------------------------------------------------------------------------------------------------------------------------------------------------------------------------------------|
| <pre> push rbp push r14 ❶ push rbx mov rbx,rdi call 401d00 <fn1@plt> ❷ mov r14,rax mov ebp,DWORD PTR [r14] ❸ test rbx,rbx mov eax,0x425530 ❹ cmove rbx,rax mov esi,0x38 ❺ mov rdi,rbx call 40a130 <fn2> ❻ ... </pre> | <pre> push_bp8/ push_reg8/ push_reg8/ mov_reg8_reg8/ call_externfunc/ mov_reg8_reg8/ mov_bp4_dwordptr[reg8]/ test_reg8_reg8/ mov_reg4_dispbss/ cmove_reg8_reg8/ mov_reg4_immval/ mov_reg8_reg8/ call_innerfunc/ ... </pre> | <pre> X_push_rbp/ X_push_r14/ X_push_rbx/ X_mov_r11d_r15d/ X_call_HIMM/ X_mov_esi_eax/ X_mov_ebp_r14*1+0/ X_test_rbx_rbx/ X_mov_eax_HIMM/ X_cmove_rbx_rax/ X_mov_esi_0x38/ ❷ X_mov_rdi_rbx/ X_call_HIMM/ ... </pre> | <pre> push/reg8/ push/reg8/ ❸ push/reg8/ mov/reg8/reg8/ call/imme/ mov/reg8/reg8/ mov/reg4/ptr/ test/reg8/reg8/ mov/eax/imme/ cmove/rbx/rax mov/reg4/imme/ mov/reg8/reg8/ call/imme/ ... </pre> | <pre> PUSHQ~RBP/ PUSHQ~R14/ PUSHQ~RBX/ MOVQ~RBX,RDI/ CALLQ~FOO/ MOVQ~R14,RAX/ MOVQ~RBP,[R14] ❺ TESTQ~RBX,RBX/ MOVQ~RAX,0/ CMOVEQ~RBX,RAX/ MOVQ~RSI,0/ MOVQ~RDI,RBX/ CALLQ~FOO/ ... </pre> |

Figure 7: Varying strategies of normalizing (disassembled) instructions prior to code embedding generation. A slash (/) represents a token separator; e.g., DeepBinDiff [77] separately tokenizes opcode and corresponding operand(s) by splitting an instruction. Note that a strategy that is too coarse-grained (e.g., DeepBinDiff [77], InnerEye [83]) may lose contextual information; on the other hand, a strategy that is too fine-grained (e.g., SAFE [49]) may suffer from an OOV problem (See §4.2).

is unable to convey a valid context. Note that the OOV problem can be minimized with our strategy.

Table 1 summarizes three basic principles in mind to balance seemingly conflicting goals above: i) an immediate can fall into a jump or call destination (e.g., ❷ `0x401d00` → `externfunc`, ❹ `0x425530` → `innerfunc`), a value itself (e.g., ❺ `0x38` → `immval`) or a reference (e.g., ❸ `0x425530` → `dispbss`), according to a string literal, statically allocated variable or other data; ii) a register can be classified with a size by default (e.g., ❶ `r14` → `reg8`, ❹ `eax` → `reg4`); but the ones with a special purpose stay intact such as a stack pointer, instruction pointer, or base pointer (e.g., ❸ `ebp` → `bp4`); and iii) a pointer expression follows the original format, “base+index*scale+displacement” (e.g., ❸ `DWORD PTR [r14]` → `dwordptr[reg8]`) so that certain memory access information can be preserved; moreover, the same rule applies if and only if the displacement refers to a string reference (e.g., `dispstr`). Note that opcode is not part of our normalization process.

4.3 Pre-training Model

It is necessary to train DEEPSemantic with a completely new dataset (e.g., machine instructions in our corpus) with an entirely different vocabulary (e.g., normalized instructions). However, in general, it is possible to employ a pre-trained model with a large corpus of human words (e.g., from Wikipedia) in an NLP domain because BERT training is not only computationally expensive but also excellent to apply to various downstream pipelines by design [64, 69, 71].

We adopt the original BERT’s masked language model (MLM) that probabilistically masks a pre-defined portion of normalized instructions (e.g., 15%), followed by predicting them in a given function during pre-training. It is noteworthy that DEEPSemantic does not employ NSP (i.e., prediction of next sentence) because two consecutive functions often do not connect semantically. We visualize the internal structure of multi-head self-attention with multiple layers in Appendix (§9) for the interested readers. Besides, our model instinctively takes advantage of Transformer (comparing to prior RNN models), which allows for direct connection between

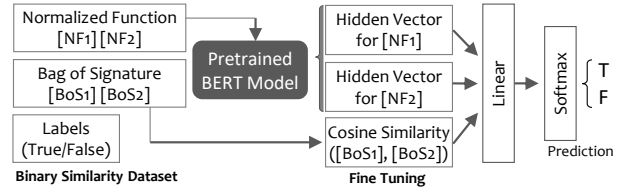


Figure 8: Binary similarity prediction model (DS-BINSIM) as a fine tuning task.

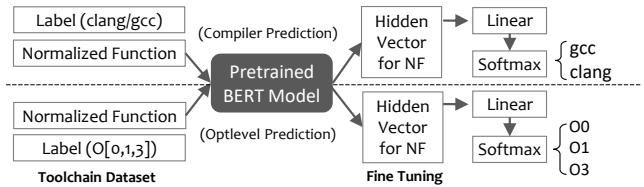


Figure 9: Toolchain (compiler and optimization level) classification model (DS-TOOLCHAIN) as a fine tuning task.

all instructions effectively, and highly parallelizable computation (e.g., GPU resource).

4.4 Fine-tuning Model

DEEPSemantic aims to support specific downstream tasks that need to infer contextual information of a binary code with a relatively quick re-training based on a pre-trained model for generic code representation. A fine-tuning stage requires another dataset preparation with a label (supervised learning) to learn a specific task. In this paper, we define two downstream tasks to demonstrate the effectiveness of our model: a binary similarity (DS-BINSIM) task that predicts whether two functions are similar and a toolchain prediction task (DS-TOOLCHAIN) that classifies either a compiler or optimization level.

4.4.1 DS-BINSIM Model. We define our first downstream task as estimating the similarity of two binary functions that originate

| Operand | Rule | Description or Expression | Notation | Note |
|-----------------------|-------------------------|-----------------------------------------------------|--------------------------------------|---------------------------------------------|
| Immediate | call target | libc library call | libc[name] | points to a libc function |
| | | recursive call | self | points to a function itself |
| | | function call within a binary | innerfunc | points to a .text section |
| | | function call out of a binary | externfunc | points to a .got or .plt section |
| | jump family | destination to jump to | jmpdst | destination within a function |
| reference | string | statically allocated variables | dispstr | refers to a string |
| | | data | dispbss | points to a .bss section |
| | default | all other immediate values | dispdata | refers to data other than a string |
| Register | default | all other immediate values | immval | all cases other than the above |
| | size | $[e r]^*[a b c d s i di][x h]^*, r[8-15][b w d]^*$ | reg[1 2 4 8] | size information |
| | stack/base/instruction | $[e r]^*[b s i]p[1]^*$ | [s b i]p[1 2 4 8] | special registers (e.g., stack) |
| | special purpose | cr[0-15], dr[0-15], st([0-7]), [c d e f g s]s | reg[cr dr st], reg[c d e f s]s | special registers (e.g., flags) |
| special purpose (avx) | $[x y z]^*mm[0-7]0-31]$ | reg[x y z]^*mm | Advanced vector extensions registers | |
| Pointer | direct (small size) | byte,word,dword,qword,ptr | memptr[1 2 4 8] | pointer with a small size (≤ 8 bytes) |
| | direct (large size) | tbyte,xword,[x y z]mmword | memptr[10 16 32 64] | pointer with a large size (> 8 bytes) |
| | indirect (string) | $[base+index*scale+displacement]$ | $[base+index*scale+dispstr]$ | pointer that refers to a string |
| | indirect (others) | $[base+index*scale+displacement]$ | $[base+index*scale+disp]$ | pointer with a displacement |

Table 1: Well-balanced normalization rules for the representation of x86_64 instruction operands: immediate, register and pointer. Our strategy aims to remain as much contextual information as possible for further embedding generation.

from the same source code. We define a new dataset that comprises two normalized functions (NFs) with a label (whether an identical function pair). Figure 8 illustrates our binary similarity model as a downstream task. We load DS-PRE as a basis to obtain two hidden vectors (size= h) from each NF. Note that we also include supplementary information, dubbed *Bag of Signature (BoS)*³, to enhance the binary similarity task. Next, we concatenate three vectors (i.e., two hidden vectors and cosine similarity of two BoSes) and then pass them through a linear layer where the number of inputs and outputs are $2 * h + 1$ and 2, respectively.

4.4.2 DS-TOOLCHAIN Model. We define another downstream task to predict either a compiler or optimization level because recovering the toolchain provenance of binary code is an important task in the literature of digital forensics [54, 62]. Note that our model experimentally shows poor performance in categorizing both compiler and optimization together (See §6.5 in detail); hence, we separate DS-TOOLCHAIN into two sub-tasks: compiler and optimization level classification. Figure 9 depicts our model, which is simpler than DS-BINSIM. Similarly, we extract a hidden vector from each NF and then train the classifier with a linear and softmax layer.

4.4.3 Model and Loss Function. Both §4.4.1 and §4.4.2 tasks are a multi-class (including binary) classification problem. In particular, the logits of both downstream tasks can be calculated as:

$$\hat{y} = \text{Softmax}(\mathcal{F}(h)) \quad (1)$$

where $\mathcal{F}(\cdot)$ and h are a fully-connected layer and the hidden vector of the given function returned from DS-PRE, respectively. To obtain the optimal network parameters in the fine-tuning layers, we use cross-entropy as a loss function. In other words, we find the network parameters θ that satisfy:

$$\theta = \arg \min_{\theta} \sum_{c \in C} p(c|y) \log(p(c|\hat{y})) \quad (2)$$

³Feeding additional information indeed improves our model, however, the difference is marginal (0.09% as in Figure 8). Interested readers refer to Appendix (§9)

where C , $p(c|y)$, and $p(c|\hat{y})$ denote a set of classes (e.g., decision of function similarity in DS-BINSIM or toolchain prediction in DS-TOOLCHAIN), the ground-truth class distribution, and the estimated probability for the class c by the logits \hat{y} calculated from Equation 1.

5 IMPLEMENTATION

This section briefly describes the artifacts from static binary analysis and DEEPSEMANTIC implementation.

Binary Analysis Artifacts. With our corpus (Table 3), we extract essential artifacts from one of the state-of-the-art static binary analysis tools, IDA Pro 7.2 [30]. We leverage IDAPython [31] (a built-in IDA Pro [30] plugin) to build an initial database of binary analysis artifacts including function names, libc library calls, cross references (e.g., string literals, numeric constants), section names and call invocations (e.g., internal calls, external calls), which further assists achieving a well-balanced normalization process as described in Table 1. Although we provide a binary with debugging symbols available to confirm the ground truth (e.g., function boundaries) during static analysis, DEEPSEMANTIC is agnostic to the availability of such debugging information. Any binary analysis tool would suffice to recognize binary functions such as angr [8], Ghidra [52], or radare2 [60].

BERT Model without NSP. We develop DEEPSEMANTIC with Tensorflow [28] and PyTorch [59] on top of a few existing BERT implementations [29, 36, 72]. As described in §4, DEEPSEMANTIC does not compute NSP when building a language model unlike the original BERT architecture because the semantics of a function is *location-independent* from that of its adjacent functions. We pre-train with a batch size of 96 sequences, where each sequence contains 256 tokens (e.g., $256 * 96 = 24,576$ tokens/batch including special tokens) using five epochs over the 1.3M binary functions. We use the Adam optimizer with a learning rate of 0.0005, $\beta_1 = 0.9$, $\beta_2 = 0.999$, L2 weight decay rate of 0.01, and liner decay of the learning rate. We use a dropout rate of 0.1 on all layers, and ReLU activation function.

| | | | |
|----------------------------------|-----|-------------------------|----------|
| (B) Dimension of embeddings | 256 | (O) Loss rate | 0.0005 |
| (B) Number of hidden layers | 128 | (O) Adam beta1 | 0.9 |
| (B) Number of attention layers | 8 | (O) Adam beta2 | 0.999 |
| (B) Number of attention heads | 8 | (O) Adam weight decay | 0.01 |
| (B) Maximum length of encoding | 250 | (O) Adam epsilon | 1.00E-06 |
| (B) Position dropout | 0.1 | (O) Warmup | Linear |
| (B) Conv1d dropout | 0.2 | (T) Epochs | 5 |
| (B) Number of conv1d layers | 3 | (T) Batch size | 96 |
| (B) Size of conv1d kernel | 5 | (T) Train dataset ratio | 0.9 |
| (B) Feed forward network dropout | 0.1 | (T) Valid dataset ratio | 0.05 |
| (B) Self-attention dropout | 0.1 | (T) Test dataset ratio | 0.05 |

Table 2: Hyperparameters for (B)ERT, (O)ptimizer, and (T)rainer during a training phase.

Table 2 encapsulates all hyperparameters when we build our models for the BERT language model, optimizer, and trainer. The number of trainable parameters is 8, 723, 914 for DS-PRE.

6 EVALUATION

As the approach of DEEPSemantic inherently involves a training process twice – DS-PRE and DS-TASK – accordingly, we set up various experiments for accurate and fair evaluation. We first build a DS-PRE model (§6.1), followed by answering the following five research questions from three aspects: i) effectiveness (RQ1-3) that focuses on DS-BINsim, ii) applicability (RQ4) with DS-TOOLCHAIN, and iii) efficiency (RQ5) of DEEPSemantic in practice.

- **RQ1.** How much does DS-BINsim outperform existing cutting-edge approaches (e.g., DeepBinDiff [77], SAFE [49]) for a binary similarity detection task that requires the inference of underlying binary semantics (§6.2)?
- **RQ2.** How well does a fine-tuning task enhance binary code representation? We assess how DS-BINsim updates the original function embedding vectors from DS-PRE (§6.3).
- **RQ3.** How much improvement does well-balanced normalization offer for DS-BINsim model?
- **RQ4.** Can DEEPSemantic be applicable to other downstream tasks (e.g., compiler and optimization level prediction) (§6.5)?
- **RQ5.** How efficient is DEEPSemantic in practice (§6.6)?

Environment. We evaluate DEEPSemantic on a 64-bit Ubuntu 18.04 system equipped with Intel(R) i9-10900X CPU (with 20 3.70 GHz cores), 128 GB RAM and NVIDIA Quadro RTX 8000 GPU.

Dataset. Table 3 defines the whole corpus for our dataset. We generate the 1,328 binaries compiled with two compilers (e.g., gcc 5.4 and clang 6.0.1) and four optimization levels (e.g., 0[0-3]) from three different testsuites (e.g., GNUutils, SPEC2017, the utilities including openssl [53], nginx [51], and vsftpd [68]). The 176 SPEC2006 binaries are borrowed from the official release [55].

6.1 DS-PRE Generation

With the artifacts corresponding to each binary from §5, we normalize all instructions, define tokens, and create a dataset for BERT pre-training. We obtain 17,225 tokens in total from all 107.88 million instructions in our corpus including i) each instruction token (every instruction represents an individual token in our model) from a normalized instruction and ii) five special tokens ([SOS]: start of a sentence, [EOS]: end of a sentence, [UNK]: unknown token, [MASK]:

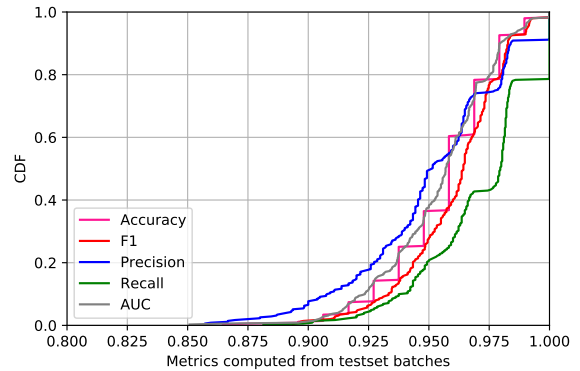


Figure 10: CDF of varying metrics to show the performance of DS-BINsim (See Table 7).

mask to predict a word, [PAD]: padding symbol to fill out an input length) for DS-PRE generation, which is a modified BERT model described in Figure 2. The total number of all normalized binary functions is 1,690,715 in our corpus; however, we solely include around 1.3 million functions after filtering out either functions that are too small (the number of instructions is less than or equal to five; 15.4%) or too large (greater than 250 instructions; 4.5%) ones.

This is because i) the BERT structure can hardly learn functions that are too small in a mask language model; e.g., we use a masking rate of 15% like the original BERT model; thus at least six instructions (as a single sentence) can play a role of a meaningful semantic chunk for training, which generates an appropriate number of masks for prediction during training, and ii) functions that are too large may hinder performance of pre-training model generation; and thus they have been excluded (4.5%). It is noteworthy that we have not excluded the identical NFs during pre-training model generation because they can be regarded as a different training dataset considering the nature of the probabilistic masking mechanism in MLM. Additionally, the ratio of OOV in the test set is around 0.93%, that is, merely 82 vocabularies are unknown out of 8,783 tokens (the number of vocabularies in the training set is 17,024).

6.2 Effectiveness of DS-BINsim

As one of downstream tasks with DEEPSemantic, this section demonstrates the effectiveness of DS-BINsim for a binary similarity task by comparing with the two state-of-the-art tools using deep learning. According to the model illustrated in Figure 8, we prepare a dataset that consists of pairs of two normalized functions (NFs), and their labels. If two binary functions are from the same source code, the label indicates 1 (true) or 0 (false) otherwise. With the same hyperparameters in Table 2, we generate a fine-tuning model (DS-BINsim) that allows for predicting binary similarity. Figure 10 illustrates the CDF of varying metrics, including an F1 of 0.965 and AUC of 0.959 on average (See other metrics in the first column in Table 7). This means our classifier can accurately make a prediction if two binary functions are compiled from the same source *regardless of* a wide range of code transformations from arbitrary combination of compilers and optimization levels.

| Testsuite | Number of Occurrence | | | | | Rate | | Metrics | | | Average Occurrence per FN | | |
|-----------|----------------------|-----------|------------|-------------|--------|-----------|-----------|---------|--------|--------|---------------------------|--------|------|
| | Binaries | FNs | BBs | INs | Vocas | Small FNs | Large FNs | BBs/FN | INs/FN | INs/BB | Immediate | String | Libc |
| GNUutils | 1,000 | 446,014 | 3,983,384 | 22,216,363 | 5,328 | 13.70% | 3.14% | 8.93 | 49.81 | 5.58 | 7.99 | 1.01 | 0.88 |
| Spec2006 | 176 | 408,496 | 4,664,973 | 28,321,431 | 9,632 | 14.96% | 5.01% | 11.42 | 69.33 | 6.07 | 9.72 | 0.81 | 0.41 |
| Spec2017 | 120 | 755,673 | 9,339,087 | 52,952,315 | 11,933 | 13.90% | 4.83% | 12.36 | 70.07 | 5.67 | 10.37 | 0.68 | 0.28 |
| Utils | 32 | 80,532 | 788,861 | 5,083,417 | 4,963 | 18.89% | 4.94% | 9.80 | 63.12 | 6.44 | 11.95 | 0.97 | 0.25 |
| Total | 1,328 | 1,690,715 | 18,776,305 | 108,573,526 | 17,220 | 15.36% | 4.48% | 10.63 | 63.08 | 5.94 | 10.01 | 0.87 | 0.46 |

Table 3: Summary of our whole corpus. FN, BB and IN represent a function, basic block and instruction, respectively. A small function indicates the number of instructions per function (I/F) is less than or equal to 5, whereas a large function indicates I/F is greater than 250. We also investigate the number of immediate operands, string references and libc call invocations per function to devise well-balanced normalization.

| Experiment | Limited Testset | | | | | | |
|------------|-----------------|-------|-------|--------------|-------|-------|--------|
| | DeepBinDiff | | | DeepSemantic | | | |
| Pair | P | R | F1 | P | R | F1 | Diff |
| (C00,C01) | 0.574 | 0.197 | 0.293 | 0.907 | 0.907 | 0.907 | 61.40% |
| (C00,C02) | 0.528 | 0.176 | 0.264 | 0.924 | 0.910 | 0.917 | 65.29% |
| (C00,C03) | 0.501 | 0.178 | 0.263 | 0.910 | 0.924 | 0.917 | 65.43% |
| (C00,G00) | 0.693 | 0.279 | 0.398 | 0.921 | 0.930 | 0.925 | 52.72% |
| (C00,G01) | 0.529 | 0.173 | 0.261 | 0.934 | 0.915 | 0.925 | 66.40% |
| (C00,G02) | 0.506 | 0.151 | 0.233 | 0.930 | 0.920 | 0.925 | 69.22% |
| (C00,G03) | 0.488 | 0.151 | 0.231 | 0.932 | 0.905 | 0.918 | 68.74% |
| (C01,C02) | 0.727 | 0.643 | 0.682 | 0.928 | 0.921 | 0.924 | 24.20% |
| (C01,C03) | 0.705 | 0.612 | 0.655 | 0.930 | 0.911 | 0.921 | 26.55% |
| (C01,G00) | 0.599 | 0.202 | 0.302 | 0.931 | 0.917 | 0.924 | 62.15% |
| (C01,G01) | 0.613 | 0.330 | 0.429 | 0.923 | 0.909 | 0.916 | 48.67% |
| (C01,G02) | 0.592 | 0.375 | 0.459 | 0.914 | 0.911 | 0.913 | 45.33% |
| (C01,G03) | 0.546 | 0.346 | 0.424 | 0.921 | 0.915 | 0.918 | 49.41% |
| (C02,C03) | 0.947 | 0.863 | 0.903 | 0.925 | 0.917 | 0.921 | 1.79% |
| (C02,G00) | 0.509 | 0.187 | 0.274 | 0.933 | 0.918 | 0.926 | 65.21% |
| (C02,G01) | 0.600 | 0.302 | 0.402 | 0.919 | 0.903 | 0.911 | 50.88% |
| (C02,G02) | 0.606 | 0.343 | 0.438 | 0.918 | 0.918 | 0.918 | 47.99% |
| (C02,G03) | 0.598 | 0.344 | 0.437 | 0.934 | 0.913 | 0.923 | 48.65% |
| (C03,G00) | 0.494 | 0.179 | 0.263 | 0.910 | 0.910 | 0.910 | 64.73% |
| (C03,G01) | 0.577 | 0.300 | 0.395 | 0.937 | 0.930 | 0.934 | 53.87% |
| (C03,G02) | 0.605 | 0.349 | 0.443 | 0.928 | 0.929 | 0.929 | 48.60% |
| (C03,G03) | 0.579 | 0.342 | 0.430 | 0.920 | 0.920 | 0.920 | 49.01% |
| (G00,G01) | 0.582 | 0.221 | 0.320 | 0.916 | 0.910 | 0.913 | 59.24% |
| (G00,G02) | 0.555 | 0.190 | 0.283 | 0.943 | 0.916 | 0.929 | 64.59% |
| (G00,G03) | 0.515 | 0.187 | 0.274 | 0.920 | 0.916 | 0.918 | 64.35% |
| (G01,G02) | 0.784 | 0.556 | 0.651 | 0.930 | 0.927 | 0.929 | 27.80% |
| (G01,G03) | 0.751 | 0.536 | 0.626 | 0.924 | 0.900 | 0.912 | 28.62% |
| (G02,G03) | 0.848 | 0.737 | 0.789 | 0.942 | 0.929 | 0.935 | 14.65% |
| Average | 0.613 | 0.337 | 0.422 | 0.925 | 0.916 | 0.921 | 49.84% |

Table 4: Precision, Recall, and F1 results of binary similarity comparison between DS-BINSIM and DeepBinDiff [77]. DS-BINSIM significantly outperforms DeepBinDiff (e.g., around 49.8%) across all pair combinations.

Comparison with DeepBinDiff. We conduct an experiment to compare DEEPSemantic with open-sourced DeepBinDiff [79]. Unfortunately, the officially released DeepBinDiff did not handle even medium-size binaries, we had no choice but to define a limited dataset (96 executables in total) including part of the SPEC2006 and findutils⁴. By design, DeepBinDiff performs basic block matching by taking two binary inputs, whereas DS-BINSIM aims for comparisons at the function granularity. In this respect, we classify

⁴astar, bzip2, hminer, lbm, libquantum, mcf, milc, namd, sphinx_livepretend, and findutils (find, xargs, locate)

| Experiment | Full Testset | | | | | | |
|------------|--------------|-------|-------|--------------|-------|-------|--------|
| | SAFE | | | DeepSemantic | | | |
| Pair | P | R | F1 | P | R | F1 | Diff |
| (C00,C01) | 0.879 | 0.728 | 0.796 | 0.958 | 0.975 | 0.967 | 17.03% |
| (C00,C02) | 0.774 | 0.676 | 0.722 | 0.973 | 0.967 | 0.970 | 24.79% |
| (C00,C03) | 0.830 | 0.627 | 0.715 | 0.958 | 0.969 | 0.963 | 24.87% |
| (C00,G00) | 0.788 | 0.996 | 0.880 | 0.955 | 0.979 | 0.967 | 8.68% |
| (C00,G01) | 0.836 | 0.704 | 0.764 | 0.943 | 0.968 | 0.956 | 16.05% |
| (C00,G02) | 0.698 | 0.662 | 0.679 | 0.940 | 0.975 | 0.957 | 27.79% |
| (C00,G03) | 0.713 | 0.648 | 0.679 | 0.945 | 0.983 | 0.963 | 28.44% |
| (C01,C02) | 0.770 | 0.824 | 0.796 | 0.954 | 0.973 | 0.963 | 16.70% |
| (C01,C03) | 0.685 | 0.824 | 0.748 | 0.963 | 0.989 | 0.976 | 22.78% |
| (C01,G00) | 0.796 | 0.794 | 0.795 | 0.954 | 0.981 | 0.967 | 17.22% |
| (C01,G01) | 0.871 | 0.955 | 0.911 | 0.942 | 0.974 | 0.958 | 4.69% |
| (C01,G02) | 0.737 | 0.882 | 0.803 | 0.954 | 0.984 | 0.969 | 16.55% |
| (C01,G03) | 0.732 | 0.909 | 0.811 | 0.949 | 0.960 | 0.955 | 14.37% |
| (C02,C03) | 0.662 | 0.978 | 0.789 | 0.959 | 0.971 | 0.965 | 17.55% |
| (C02,G00) | 0.679 | 0.689 | 0.684 | 0.951 | 0.981 | 0.965 | 28.14% |
| (C02,G01) | 0.813 | 0.952 | 0.877 | 0.968 | 0.982 | 0.975 | 9.75% |
| (C02,G02) | 0.825 | 0.942 | 0.880 | 0.965 | 0.986 | 0.975 | 9.54% |
| (C02,G03) | 0.830 | 0.949 | 0.885 | 0.939 | 0.978 | 0.958 | 7.24% |
| (C03,G00) | 0.731 | 0.746 | 0.738 | 0.945 | 0.990 | 0.967 | 22.85% |
| (C03,G01) | 0.864 | 0.941 | 0.901 | 0.950 | 0.961 | 0.955 | 5.42% |
| (C03,G02) | 0.909 | 0.961 | 0.934 | 0.948 | 0.977 | 0.962 | 2.81% |
| (C03,G03) | 0.791 | 0.966 | 0.870 | 0.947 | 0.962 | 0.954 | 8.45% |
| (G00,G01) | 0.757 | 0.802 | 0.779 | 0.964 | 0.967 | 0.966 | 18.66% |
| (G00,G02) | 0.815 | 0.687 | 0.745 | 0.953 | 0.962 | 0.958 | 21.20% |
| (G00,G03) | 0.796 | 0.651 | 0.716 | 0.955 | 0.982 | 0.968 | 25.21% |
| (G01,G02) | 0.815 | 0.993 | 0.895 | 0.961 | 0.967 | 0.964 | 6.92% |
| (G01,G03) | 0.854 | 0.944 | 0.897 | 0.961 | 0.969 | 0.965 | 6.80% |
| (G02,G03) | 0.755 | 0.938 | 0.837 | 0.949 | 0.982 | 0.965 | 12.85% |
| Average | 0.786 | 0.835 | 0.805 | 0.954 | 0.975 | 0.964 | 15.83% |

Table 5: Precision, Recall, and F1 results of binary similarity comparison between DS-BINSIM and SAFE [49]. DS-BINSIM surpasses SAFE (e.g., around 15.8%) across all pair combinations.

each case into a true positive for a fair comparison with DeepBinDiff when it discovers *any pair of matching basic blocks* that belong to the same function (relaxed judgment). It is noteworthy mentioning that we extend the evaluation of DeepBinDiff across different compilers (i.e., gcc VS clang) as well as optimization levels (i.e., 28 different combinations) to demonstrate the effectiveness of DS-BINSIM. Table 4 shows that our approach considerably outperforms DeepBinDiff (49.8%) at all combinations of compiler and optimization levels. Our experiment aligns with the results across optimizations from DeepBinDiff [77].

| Category | DS-PRE | DS-BINSIM |
|------------|--------|-----------|
| Similar | 0.647 | 0.751 |
| Dissimilar | 0.273 | 0.309 |

Table 6: Cosine similarity of similar/dissimilar function pairs on average between DS-PRE and DS-BINSIM.

Comparison with SAFE. We conduct another experiment with a full test dataset in our corpus to compare with SAFE [49]. By design, SAFE merely computes a cosine similarity value rather than making a decision on (True/False). Hence, we found a threshold of 0.5 (*i.e.*, if the value is larger than the threshold, the decision is true) where SAFE gives us the best performance. To this end, we create a database for our whole dataset (Table 3) to query a function embedding with the open-sourced version of SAFE [47]. Table 5 demonstrates that our approach surpasses SAFE (15.8%) on the full testset. In particular, we observe a substantial difference when code semantics is more difficult to infer (*e.g.*, high optimization level difference).

Answer to RQ1. DS-BINSIM by far outperforms DeepBinDiff (up to 69%) and SAFE (up to 28%) across all 28 combinations of different compilers and optimization levels.

6.3 Code Representation with Fine-Tuning

We assess whether a 256-dimensional embedding (Table 2) that represents a function can be updated after fine-tuning. It is worth noting that there are several ways to extract a contextualized embedding [7]; here we use a mean of all hidden states.

To this end, we extract 179,163 unique function pairs from our corpus including approximately half for similar ones and another half for dissimilar ones, and then compute cosine similarity scores. Note that we exclude all obvious cases in which two NFs are exactly identical because the score becomes 1 at all times. For example, the similarity score of the similar function embedding pair, `ngx_resolver_resend_handler` between the clang O1 (70 instructions) and gcc O2 (86 instructions) is 0.805 with the DS-PRE model. After fine-tuning with the DS-BINSIM model, we obtain an improved similarity value of 0.826 for the above example, indicating the vectorized values for the similar pair is close to 1. Table 6 briefly shows cosine similarity values on average. We observe that the binary function representation have been enhanced; *i.e.*, the difference between the similar pairs in a vector space become broader on average.

Answer to RQ2. Our empirical results indicate that a fine-tuning process successfully updates code representations for a specific task (*e.g.*, DS-BINSIM).

6.4 Effectiveness of Well-balanced Normalization

This section depicts how well-balanced normalization with pre-defined rules (Table 1) enhances DS-BINSIM. To assess its effectiveness, we attempt to compare DEEPSemantic with a fine-grained model without normalization (note that the only rule applied is replacing every immediate operand with `immval`). With our corpus, the number of tokens is 4,917,904 in a training set, which is 207.4 times bigger than well-balanced normalization, requiring

| Metric | Normalization Granularity | | | Bag of Signature (BoS) | | |
|-----------|---------------------------|--------|---------|------------------------|---------|---------|
| | Balanced | Coarse | (Diff) | With | Without | (Diff) |
| FPR | 0.057 | 0.110 | -5.250% | 0.058 | 0.059 | -0.109% |
| TPR | 0.975 | 0.962 | 1.347% | 0.974 | 0.973 | 0.075% |
| Accuracy | 0.961 | 0.934 | 2.712% | 0.960 | 0.959 | 0.101% |
| Precision | 0.955 | 0.932 | 2.323% | 0.954 | 0.953 | 0.093% |
| Recall | 0.975 | 0.962 | 1.347% | 0.974 | 0.973 | 0.075% |
| F1 | 0.965 | 0.946 | 1.869% | 0.964 | 0.963 | 0.088% |
| AUC | 0.959 | 0.926 | 3.299% | 0.958 | 0.957 | 0.091% |

Table 7: Metric comparison to show the effectiveness of well-balanced normalization and BoS for model generation. Supplementary information clearly enhances the final model.

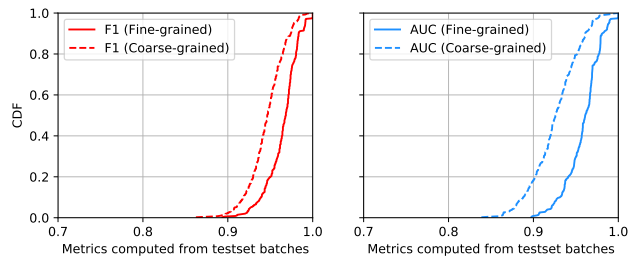


Figure 11: CDF comparison of F1 and AUC metrics between coarse-grained (dotted lines) and well-balanced normalization (solid lines).

283.6 GB GPU memory to update 1.38 billion trainable parameters. The problem has been exacerbated as well as a resource constraint considering that most of vocabularies (3,716,287 or 75.6%) appear only once, failing to update corresponding instruction vectors while training. Moreover, 97.8% (127,805 out of 130,736) of all tokens in the test set are not shown in the training set, rendering further learning pointless due to a severe OOV problem (*i.e.*, most of vocabularies would be regarded as UNK).

Next, we set up our experiment by re-defining a relatively coarse-grained normalization rule; simply put, all immediates and pointers have been replaced with `immval` and `ptr` without taking any information into account (we merely include a normalization rule for registers), followed by generating a new dataset (1,174,060 functions). This conversion shrinks the number of tokens up to 2,022 including five special ones from 17,225 of well-balanced normalization (around 88.3% reduction). We generate another DS-PRE model for coarse-grained normalization with 2,870,759 trainable parameters. Then, we prepare another DS-BINSIM dataset with labels, taking 100K pairs (the ratio of similar and dissimilar labels are close to 1:1) from our corpus. It is worth noting that we exclude all identical NF pairs for similar pairs (*e.g.*, all pairs should have at least one or more discrepancies) to compute a robust model. We use negative sampling for dissimilar pairs.

As a result, we obtain higher F1 and AUC values of (0.965, 0.959) with well-balanced normalization than those of (0.946, 0.926) with coarse-grained normalization (See Table 7). Figure 11 shows that the case applying well-balanced normalization has better F1 by 1.87% and AUC by 3.30%. Notably, well-balanced normalization decreases the false positive rate by 5.25%. Although the margins do

| Metrics | Compiler | Optlevel | Optlevel (gcc) | Optlevel (clang) |
|-----------|----------|----------|----------------|------------------|
| Precision | 0.973 | 0.913 | 0.964 | 0.873 |
| Recall | 0.972 | 0.911 | 0.964 | 0.863 |
| F1 | 0.962 | 0.910 | 0.963 | 0.862 |

Table 8: Metrics of DS-TOOLCHAIN classifiers: compiler and optimization levels (e.g., gcc and clang).

not make surprisingly high improvement, we believe that it may be fruitful for other downstream tasks that are contextually sensitive.

Answer to RQ3. Well-balanced normalization can enrich code representation by feeding supplementary information. We experimentally validate that the normalization process is essential for efficient learning toward semantic-aware code representation.

6.5 DS-TOOLCHAIN Assessment

This section introduces another useful downstream task of DEEPSemantic, that is, a classifier for a compiler or optimization level when an NF is given. Similar to previous experiments, we generate a dataset that contains all six combinations of two compilers and three optimization levels with the same rate (e.g., 106K functions per each), followed by splitting it into (train, valid, test)=(0.90, 0.05, 0.05). We rule out -02 based on our observation that a large number of NFs remain identical between -02 and -03 in clang, and -01 and -02 in gcc. This is partially because a function inlining optimization drastically transforms its shape⁵, and additional optimizations do not affect the function structure much. According to our experiment, identical NF pairs with different labels confused our classifier, resulting in a poor performance.

We generate two DS-TOOLCHAIN models (Figure 9), for compiler and optimization level prediction because our model empirically shows a low performance when attempting to categorize both compiler and optimization simultaneously. Table 8 summarizes our results; an F1 of 0.96 and 0.91 for compiler and optimization classification. We additionally carry out an experiment for optimization prediction per each compiler, resulting in a 8.5% (F1) better performance with gcc. As a similar setting⁶, O-glassesX [54] achieves an accuracy of 0.956 with an 16-instruction fixed input for predicting compiler provenance, which shows comparable performance.

Answer to RQ4. We showcase another downstream task, DS-TOOLCHAIN, which successfully classifies a compiler and optimization level with a high precision and recall.

6.6 Efficiency of DEEPSemantic

In this section, we exhibit the efficiency of DEEPSemantic in terms of practicality. Table 9 concisely shows a computational resource on average including i) duration of pre-training, fine-tuning, and testing a model per epoch and batch, and ii) GPU memory consumption for each job. Creating an initial DS-PRE model takes the longest amount of time while fine-tuning consumes relatively less expensive resources. Once training is complete, testing can be done much faster for processing (e.g., 194x faster than DS-PRE generation). Generally, GPU memory consumption may vary depending

⁵clang performs function inlining in -02 whereas gcc in -01 by default.

⁶O-glassesX [54] introduces a classifier with 19 labels using four compilers, two optimization levels (i.e., zero or max), and two architectures (i.e., x86 and x86_64).

| Metrics | Pre-training DS-PRE | Fine-tuning DS-BINSIM | Fine-tuning DS-TOOLCHAIN | Training DS-BINSIM | Training DS-TOOLCHAIN |
|---------------------|---------------------|-----------------------|--------------------------|--------------------|-----------------------|
| Per Epoch (seconds) | 3553.11 | 2229.10 | 991.87 | 43.52 | 18.25 |
| Per Batch (seconds) | 0.32 | 0.35 | 0.20 | 0.12 | 0.06 |
| GPU (GB) | 34.75 | 37.27 | 12.91 | 37.27 | 12.91 |

Table 9: Comparison of computational resources across stages (i.e., training, testing) and sub-tasks (i.e., DS-BINSIM, DS-TOOLCHAIN).

on different hyperparameter settings (e.g., batch size, the number of attention/hidden layers, maximum length of input).

Answer to RQ5. DEEPSemantic can be an efficient solution to be applicable for subtasks by carefully designing a fine-tuning model and preparing a corresponding dataset in practice.

7 DISCUSSION AND LIMITATION

This section discusses several cases to consider, feasible applications for future research, and limitations of our work.

Function Inlining and Splitting. Optimization technique sometimes involves with function inlining (i.e., a function is part of another for performance) during compilation. This means that our labels in the binary similarity classification problem may be slightly distorted with the presence of inlining and splitting. Say, a binary compiled with -03 has Function A that includes Function B where the one with -00 has both Function A and B. The function name A has not been changed but the actual content (i.e., instructions) could have in the highly optimized binary. In a similar vein, it may happen in case that a function has been separated at compilation.

Comparison Granularity. Although most of functions consist of four basic blocks or 25 instructions on average (Figure 4), there are indeed functions with a large size (as a long tail). In such cases, comparison at the basic block level would be more appropriate to seek similar blocks as demonstrated in prior work [77, 78].

Applicable Downstream Tasks. DEEPSemantic aims to support a wide range of other downstream tasks that require semantic-aware code representation by design, including (but not limited to) a special type of vulnerability scanning, software plagiarism detection, malware behavior detection, malware family classification, and bug patch detection. One can also think of identifying a function or library in a database like IDA FLIRT [32].

Normalization for Rarely Appeared Instructions. As a rule of thumb, the embedding of an instruction that has been rarely seen during pre-training may have been hardly updated (e.g., close to an initial value). Around 8.5% of the whole 17,221 normalized instructions appear only once in the corpus, as illustrated in Figure 3. Namely, such instruction embeddings may not represent a meaningful context unless the number of occurrences is sufficient.

Room for Enhancement. We thoughtfully design well-balanced normalization (Table 1), however, there are different ways of instruction normalization such as tokenization of separate opcode and operands. Besides, the BERT architecture can be replaced with others like RoBERTa [45] or XLNet [75] that has been reported better performance in popular NLP tasks, remaining as part of our future work.

Limitations. First, the current version of DEEPSemantic targets merely benign binaries. Hence, it may not be possible to directly apply DEEPSemantic to a downstream task pertaining to malware that often ships with various packing, obfuscation or encryption. Second, we have not yet tested DEEPSemantic with cross-architecture, which we leave as part of our future work. Third, one may argue binary corpus representativeness with a limited number of binaries due to the nature of software diversity. However, we carefully chose our corpus that encompasses varying sizes, types (e.g., executable, library), functionalities (e.g., compiler, interpreter, compression, server, benchmark, AI-relevant code), and languages (e.g., C/C++/Fortran). Fourth, it is possible that two different functions may have identical instructions after a normalization process, albeit a rare case. Such samples (*i.e.*, same functions with different labels) may confuse the current DEEPSemantic when building a model. Lastly, we also observe that a different set of corpora and hyperparameter settings during pre-training may impact overall performance to a downstream task.

8 RELATED WORK

Penetrating the characteristics of a machine-interpretable binary code can be applied to a wide range of real-world applications including i) code clone (software plagiarism) or similarity detection [20, 21, 23, 24, 46, 49, 61, 76–78, 80, 83], ii) malware family classification [34], detection [11, 12, 41], and analysis [38, 42, 81], iii) authorship prediction [37, 43], iv) known bug discovery (code search) [13–15, 25, 44, 48, 57, 58, 63, 65], v) patching analysis [26, 35, 73], and vi) toolchain provenance [54, 62], most of which pertain to binary similarity comparison. Here we categorize such efforts into two approaches based on the one with or without a machine learning technique.

Deterministic Approaches. Static and dynamic analyses are two mainstream techniques to learn the underlying semantics of a binary code. Luo et al. [46] introduce a means to detect cloned code with the longest common subsequence of semantically equivalent basic blocks. In a similar vein, Esh [20] leverages data-flow slices of basic blocks to detect binary similarity, and later extending the idea through re-optimization [21] to improve performance. Blanket execution [24] takes an approach of a dynamic equivalence testing primitive by defining seven major features. Malware research has largely adopted deterministic approaches including i) malware classification by extracting static features [34], ii) malware detection with structural similarities between multiple mutations [41] or control-flow graph matching [11, 12], and iii) malware authorship inference [37, 43]. Meanwhile, varying approaches have been proposed in the field of known bug discovery by leveraging i) a tree edit distance between the signature of a target basic block and that of other basic blocks [58], ii) the input/output behavior of basic blocks from intermediate representation lifting [57], and iii) dissimilar code filtering with manual features such as numeric and structural information [25]. Further, Genius [65] and FERMA-DYNE [15] devise another bug search engine for IoT firmware with both statistical and structural features where BinGo [13] supports both cross-architecture and cross-OS with a selective inlining technique to capture function semantics. Oftentimes, static analysis suffers from scalability (*e.g.*, expensive graph matching algorithm,

path explosion) or flexibility from a structural difference (*e.g.*, optimization), while dynamic analysis struggles with incomplete code coverage (*e.g.*, relying on inputs) and behavior undecidability.

Probabilistic Approaches. Recent advancements with machine learning techniques have received much attention to be applicable for binary analysis, fulfilling both effectiveness and efficiency. Malware analysis is one of popular applications: i) BinDNN [42] is one of the early works to leverage deep neural networks (*e.g.*, LSTM) to function matching for malware, ii) Zhang et al. [81] present dynamic malware analysis with feature engineering (API calls), and iii) Neurlux [38] proposes a system that learns features from a dynamic analysis report (*i.e.*, behavioral information of malware) automatically. Code similarity detection is another active domain using a probabilistic approach. Gemini [76] presents a cross-platform binary code similarity detection with a graph embedding network and Siamese network [10]. Lately, varying efforts to deduce underlying semantics of a binary code have been made with *deep learning*. InnerEye [83] aims to detect code similarity across different architectures, borrowing the concept of neural machine translation (NMT) from an NLP domain. It generates vocabulary embeddings with a Word2vec Skipgram [50] model with a coarse-grained normalization process. Similarly, MIRROR [80] presents an idea of basic block embedding across different ISAs that utilizes an NMT model to establish the connection between the two ISAs. Asm2vec [23] takes a PV-DM model for code clone search, demonstrating that a code representation can be robust over compiler optimization and even code obfuscation. SAFE [49] generates function embedding based on a self-attentive neural network. DeepBinDiff [77] performs a binary similarity task at the basic block granularity with token embeddings for semantic information, feature vectors, and TADW algorithm for program-wide contextual information. Our experiment includes the two state-of-the-art approaches from SAFE and DeepBinDiff for comparison. Meanwhile, Redmond et al. [61] investigate the graph embedding network that extracts relevant features automatically, resulting in similar performance compared to the architecture without using any structural information, which aligns our insights. Note that DEEPSemantic use limited call graph information (*e.g.*, libc call).

Comparison with the Previous Study. *Order matters* [78] is one of the closest work with ours in terms of adopting the BERT architecture. The main difference is that *Order matters* suggests the model that represents vectors for different binaries (*i.e.*, identical source but dissimilar binaries due to different platform and optimization) as close as possible with a focus on seeking an identical binary. On the other hand, we propose the model that performs contextual similarity detection between binary functions. For evaluation, *Order matters* employs rank-aware metrics such as Top1 (according to their evaluation, they obtained 74% accuracy), MRR (Mean Reciprocal Rank) and NDCG (Normalized Discounted Cumulative Gain), whereas ours employ a classification metric. In this regard, the comparison through an experiment with *Order matters* would be the best way to show the performance of DEEPSemantic. However, we were unable to acquire the source code as it is close-sourced⁷, failing to construct an implementation based on the given

⁷The authors refused to offer the source code.

conceptual information [78] due to the absence of implementation details (e.g., model hyperparameters).

9 CONCLUSION

In this paper, we propose the DEEPSemantic architecture with BERT that allows for generating semantic-aware binary code representation. We carefully design well-balanced normalization for binary instructions to convey as much information as possible during a learning process with BERT. Moreover, our architecture leverages the original BERT design to support varying downstream tasks that require the inference of code semantics once a pre-trained model for generic code representation is readily available. Our experimental results from the two tasks demonstrate that DS-BinSIM surpasses the performance of existing binary similarity comparison tools, and DS-Toolchain also shows acceptable outcomes. We hope to aid further applications with the idea of DEEPSemantic.

REFERENCES

- [1] 2013. *Proceedings of the 22nd USENIX Security Symposium (Security)*. Washington, DC.
- [2] 2016. *Proceedings of the 23rd Annual Network and Distributed System Security Symposium (NDSS)*. San Diego, CA.
- [3] 2018. *Proceedings of the 33rd IEEE/ACM International Conference on Automated Software Engineering (ASE)*. Montpellier, France.
- [4] 2019. *Proceedings of the 2nd Workshop on Binary Analysis Research (BAR)*. San Diego, CA.
- [5] 2020. *Proceedings of the 34th AAAI Conference on Artificial Intelligence (AAAI)*. New York, NY.
- [6] 2020. *Proceedings of the 3rd Workshop on Binary Analysis Research (BAR)*. San Diego, CA.
- [7] Jay Alamar. 2018. The Illustrated BERT, ELMo, and co. (How NLP Cracked Transfer Learning). (2018). <https://jalamar.github.io/illustrated-bert/>.
- [8] Angr. 2016. Python Framework for Analyzing Binaries. (2016). <https://angr.io/>.
- [9] Dzmitry Bahdanau, Kyung Hyun Cho, and Yoshua Bengio. 2015. Neural Machine Translation by Jointly Learning to Align and Translate. In *Proceedings of the 3rd International Conference on Learning Representations (ICLR)*.
- [10] Jane Bromley, Isabelle M Guyon, Yann LeCun, Eduard Säckinger, and Roopak Shah. 1993. Signature Verification using a Siamese Time Delay Neural Network. In *Proceedings of the 6th Conference on Neural Information Processing Systems (NeurIPS)*.
- [11] Danilo Bruschi, Lorenzo Martignoni, and Mattia Monga. 2006. Detecting Self-mutating Malware Using Control-flow Graph Matching. In *Proceedings of the 3rd Conference on Detection of Intrusions and Malware and Vulnerability Assessment (DIMVA)*. Berlin, Germany.
- [12] Silvio Cesare, Yang Xiang, and Wanlei Zhou. 2014. Control Flow-Based Malware Variant Detection. *IEEE Transactions on Dependable and Secure Computing (TDSC)* (2014).
- [13] Mahinthan Chandramohan, Yinxing Xue, Zhengzi Xu, Yang Liu, Chia Yuan Cho, and Tan Hee Beng Kuan. 2016. BinGo: Cross-Architecture Cross-OS Binary Search. In *Proceedings of the 24th ACM SIGSOFT Symposium on the Foundations of Software Engineering (FSE)*. Seattle, WA.
- [14] Mahinthan Chandramohan, Yinxing Xue, Zhengzi Xu, Yang Liu, Chia Yuan Cho, and Tan Hee Beng Kuan. 2018. VulSeeker: a semantic learning based vulnerability seeker for cross-platform binary, See [3].
- [15] Daming D. Chen, Manuel Egele, Maverick Woo, and David Brumley. 2016. Towards Automated Dynamic Analysis for Linux-based Embedded Firmware, See [2].
- [16] Kyunghyun Cho, Bart van Merriënboer, Caglar Gulcehre, Dzmitry Bahdanau, Fethi Bougares, Holger Schwenk, and Yoshua Bengio. 2014. Learning Phrase Representations using RNN Encoder-Decoder for Statistical Machine Translation. In *Proceedings of the 2014 Conference on Empirical Methods in Natural Language Processing (EMNLP)*.
- [17] Yoon-Ho Choi, Peng Liu, Zitong Shang, Haizhou Wang, Zhilong Wang, Lan Zhang, and Junwei Zhou. 2020. Using Deep Learning to Solve Computer Security Challenges: a Survey. *Cybersecurity* (2020).
- [18] Andrew M. Dai and Quoc V. Le. 2015. Semi-supervised Sequence Learning. *arXiv preprint arXiv:1511.01432* (2015). <https://arxiv.org/abs/1511.01432>
- [19] Andrew M. Dai and Quoc V. Le. 2019. A Survey of Binary Code Similarity. *arXiv preprint arXiv:1909.11424* (2019). <https://arxiv.org/pdf/1909.11424.pdf>
- [20] Yaniv David, Nimrod Partush, and Eran Yahav. 2016. Statistical Similarity of Binaries. In *Proceedings of the 2016 ACM SIGPLAN Conference on Programming Language Design and Implementation (PLDI)*. Santa Barbara, CA.
- [21] Yaniv David, Nimrod Partush, and Eran Yahav. 2017. Similarity of binaries through re-optimization. In *Proceedings of the 2017 ACM SIGPLAN Conference on Programming Language Design and Implementation (PLDI)*. Barcelona, Spain.
- [22] Jacob Devlin, Ming-Wei Chang, Kenton Lee, and Kristina Toutanova. 2019. BERT: Pre-training of Deep Bidirectional Transformers for Language Understanding. In *Proceedings of the 2019 Conference of the North American Chapter of the Association for Computational Linguistics: Human Language Technologies, Volume 1 (Long and Short Papers)*. Minneapolis, Minnesota, 4171–4186.
- [23] Steven H. H. Dinga, Benjamin C. M. Fung, and Philippe Charland. 2019. Asm2vec: Boosting static representation robustness for binary clone search against code obfuscation and compiler optimization. In *Proceedings of the 40th IEEE Symposium on Security and Privacy (Oakland)*. San Francisco, CA.
- [24] Manuel Egele, Maverick Woo, Peter Chapman, and David Brumley. 2014. Blanket Execution: Dynamic Similarity Testing for Program Binaries and Components. In *Proceedings of the 23rd USENIX Security Symposium (Security)*. San Diego, CA.
- [25] Sebastian Eschweiler, Khaled Yakdan, and Elmar Gerhards-Padilla. 2016. discoverE: Efficient Cross-Architecture Identification of Bugs in Binary Code, See [2].
- [26] Halvar Flake. 2004. Structural Comparison of Executable Objects. In *Proceedings of the 1st Conference on Detection of Intrusions and Malware and Vulnerability Assessment (DIMVA)*. Dortmund, Germany.
- [27] Seyed Mohammad Ghaffarian and Hamid Reza Shahriari. 2017. Software Vulnerability Analysis and Discovery Using Machine-Learning and Data-Mining Techniques: A Survey. *Comput. Surveys* (2017).
- [28] Google. 2020. End-to-end open source machine learning platform. (2020). <https://tensorflow.org>.
- [29] Google. 2020. Release of BERT Models. (2020). <https://github.com/google-research/bert>.
- [30] Hex-Rays. 2005. IDA Pro Disassembler. (2005). <https://www.hex-rays.com/products/ida/>.
- [31] Hex-rays. 2019. IDAPython Documentation. (2019). https://www.hex-rays.com/products/ida/support/idadpython_docs/.
- [32] Hex-Rays. 2020. IDA Pro Fast Library Identification and Recognition Technology. (2020). <https://www.hex-rays.com/products/ida/tech/flirt/>.
- [33] Sepp Hochreiter and Jürgen Schmidhuber. 1997. Long Short-Term Memory. *Neural Computation* 9, 8 (1997), 1735–1780.
- [34] Xin Hu, Sandeep Bhatkar, Kent Griffin, and Kang G. Shin. 2013. MutantX-S: Scalable Malware Clustering Based on Static Features, See [1].
- [35] Yikun Hu, Yuanyuan Zhang, Juanru Li, and Dawu Gu. 2016. Cross-architecture Binary Semantics Understanding via Similar Code Comparison. In *Proceedings of the 2016 IEEE 23rd International Conference on Software Analysis, Evolution, and Reengineering (SANER)*.
- [36] huanghonggit. 2019. BERT MLM with Pytorch. (2019). <https://github.com/huanghonggit/Mask-Language-Model>.
- [37] Jiyong Jang, Maverick Woo, , and David Brumley. 2013. Towards Automatic Software Lineage Inference, See [1].
- [38] Chani Jindal, Christopher Salls, Hojjat Aghakhani, Keith Long, Christopher Kruegel, and Giovanni Vigna. 2019. Neurlux: Dynamic Malware Analysis Without Feature Engineering. In *Proceedings of the Annual Computer Security Applications Conference (ACSAC)*.
- [39] Andrej Karpathy. 2015. The Unreasonable Effectiveness of Recurrent Neural Networks. (2015). <http://karpathy.github.io/2015/05/21/rnn-effectiveness>.
- [40] TaeGuen Kim, Yeo Reum Lee, BooJoong Kang, and Eul Gu Im. 2019. Binary Executable File Similarity Calculation using Function Matching. *The Journal of Supercomputing* (2019).
- [41] Christopher Kruegel, Engin Kirda, Darren Mutz, William Robertson, and Giovanni Vigna. 2005. Polymorphic Worm Detection Using Structural Information of Executables. In *Proceedings of the 8th International Symposium on Research in Attacks, Intrusions and Defenses (RAID)*. Seattle, WA.
- [42] Nathaniel Lageman, Eric D. Kilmer, Robert J. Walls, and Patrick D. McDaniel. 2016. BinDNN: Resilient Function Matching Using Deep Learning. In *Proceedings of the 12th Security and Privacy in Communication Networks (SECOMM)*. Guangzhou, China.
- [43] Marina Lindorfer, Alessandro Di Federico, Federico Maggi, Paolo Milani Comparetti, and Stefano Zanero. 2012. Lines of Malicious Code: Insights Into the Malicious Software Industry. In *Proceedings of the Annual Computer Security Applications Conference (ACSAC)*.
- [44] Bingchang Liu, Wei Huo, Chao Zhang, Wenchao Li, Feng Li, Aihua Piao, and Wei Zou. 2018. α Diff: Cross-version Binary Code Similarity Detection with DNN, See [3].
- [45] Yinhan Liu, Myle Ott, Naman Goyal, Jingfei Du, Mandar Joshi, Danqi Chen, Omer Levy, Mike Lewis, Luke Zettlemoyer, and Veselin Stoyanov. 2019. RoBERTa: A Robustly Optimized BERT Pretraining Approach. *CoRR abs/1907.11692* (2019). <http://arxiv.org/abs/1907.11692>
- [46] Lannan Luo, Jiang Ming, Dinghao Wu, Peng Liu, and Sencun Zhu. 2014. Semantics-Based Obfuscation-Resilient Binary Code Similarity Comparison with

eight heads. In this case, the first Head of the third Layer pays an attention on two words ([CLS] and [SEP]) as keys for predicting `add_reg8_reg4` as a query. Note that [CLS] and [SEP] in the original BERT correspond to our [SOS] and [EOS].

Word prediction, under the hood, can be achieved with keys (k ; previous words), values (v ; quantities that represent the content of the words) and a query (q ; words to predict), obtaining the attention distribution of previous words (a_i) and finally computing a hidden state by maximizing the distribution as Equation 3 (d_k ; dimension of key vectors):

$$a_i = \text{softmax}\left(\frac{QK^T}{\sqrt{d_k}}\right), \text{Attention}(Q, K, V) = \sum_i a_i V_i \quad (3)$$

Bag of Signature (BoS) as Supplementary Information. The idea behind BoS is that even a well-balanced normalization process (Table 1) abandons a string or numeric constant itself that may be fruitful to better understand the context of a function, as explained in §4.1. We devise the notion of BoS, which assists a binary similarity prediction classifier by feeding additional information to our neural network. Indeed, a number of prior approaches [15, 24, 65] emphasize that such constants come into play as important feature vectors to identify the behavior of a basic block or function. We enumerate both string literals and numeric constants via static analysis, combining them into a single bag that can be used as a unique signature per each function. We can simply compute a BoS similarity score with Equation 4. As a concrete example, a function (v) contains a list of [1, 0x12, 8, 8, 8, 'Hello'] (five numeric constants with three unique values, and one string constant), whereas another function (w) holds [0x12, 8, 8, 'Hello']. Then, we can represent each vector based on counting those constants: $v = (1, 1, 3, 1)$ and $w = (0, 1, 2, 1)$ whose cosine similarity becomes 0.943.

$$\text{BoS}(\vec{v}, \vec{w}) = \frac{\vec{v} \cdot \vec{w}}{|\vec{v}| |\vec{w}|} = \frac{\sum_{i=1}^n v_i w_i}{\sqrt{\sum_{i=1}^n v_i^2} \sqrt{\sum_{i=1}^n w_i^2}} \quad (4)$$

For evaluation, we generate another model by defining a new dataset that contains meaningful BoS information (*e.g.*, the number of the BoS list is greater than or equal to five) because functions in a small size may not contain a numeric constant or string reference, as illustrated in Table 3 and Figure 4. Our results demonstrate a marginal 0.09% enhancement in both F1 and AUC. We reason that i) approximately two-thirds of binary functions in our corpus do not hold information such as immediate operands or string literals and ii) BoS has been concatenated as a single dimensional vector (after computing cosine similarity) with two hidden vectors (*e.g.*, 256 dimensions) from NFs, restricting a positive impact. While the additional information has contributed to our model with a slight margin, it indicates the model would still be efficient even when such knowledge is unavailable.

| Rank | Normalized Instruction | Ratio | Cumulative | Group | Rank | Normalized Instruction | Ratio | Cumulative | Group |
|------|--------------------------------|--------|------------|-------|------|----------------------------------|--------|------------|-------|
| 1 | mov_reg8_reg8 | 5.243% | 8.24% | M | 73 | movzx_reg4_wordptr[reg8] | 0.163% | 76.04% | M |
| 2 | call_innerfunc | 5.735% | 13.98% | C | 74 | sub_reg4_immval | 0.163% | 76.20% | |
| 3 | mov_reg8_qwordptr[bp8-disp] | 4.164% | 18.14% | M | 75 | mov_dwordptr[bp8-disp]_immval | 0.157% | 76.36% | M |
| 4 | je_jmpdst | 3.925% | 22.07% | J | 76 | mov_qwordptr[ip8+disp]_reg8 | 0.156% | 76.51% | M |
| 5 | jmp_jmpdst | 3.859% | 25.93% | J | 77 | mov_qwordptr[sp8+disp]_immval | 0.154% | 76.67% | M |
| 6 | mov_reg4_immval | 3.486% | 29.41% | M | 78 | cmp_qwordptr[bp8-disp]_immval | 0.153% | 76.82% | |
| 7 | jne_jmpdst | 2.613% | 32.03% | J | 79 | mov_qwordptr[reg8+8]_reg8 | 0.151% | 76.97% | M |
| 8 | mov_reg8_qwordptr[reg8+disp] | 2.267% | 34.29% | M | 80 | mov_qwordptr[sp8+8]_reg8 | 0.151% | 77.12% | M |
| 9 | pop_reg8 | 1.936% | 36.23% | | 81 | cmp_dwordptr[bp8-disp]_immval | 0.151% | 77.27% | |
| 10 | mov_reg4_reg4 | 1.860% | 38.09% | M | 82 | mov_reg4_bp4 | 0.150% | 77.42% | M |
| 11 | push_reg8 | 1.844% | 39.93% | | 83 | cdqe | 0.146% | 77.57% | |
| 12 | mov_qwordptr[bp8-disp]_reg8 | 1.839% | 41.77% | M | 84 | test_reg1_immval | 0.141% | 77.71% | |
| 13 | xor_reg4_reg4 | 1.725% | 43.50% | | 85 | jg_jmpdst | 0.140% | 77.85% | J |
| 14 | ret | 1.477% | 44.97% | C | 86 | mov_reg8_sp8 | 0.139% | 77.99% | M |
| 15 | test_reg8_reg8 | 1.387% | 46.36% | | 87 | mov_reg4_dispbss | 0.137% | 78.13% | M |
| 16 | mov_reg8_qwordptr[reg8] | 1.370% | 47.73% | M | 88 | shr_reg4_immval | 0.136% | 78.26% | |
| 17 | mov_reg8_qwordptr[sp8+disp] | 1.306% | 49.04% | M | 89 | mov_reg8_qwordptr[reg8+reg8*8] | 0.134% | 78.40% | M |
| 18 | cmp_reg4_immval | 1.111% | 50.15% | | 90 | mov_reg8_qwordptr[sp8] | 0.134% | 78.53% | M |
| 19 | add_reg8_immval | 1.107% | 51.25% | | 91 | call_reg8 | 0.132% | 78.66% | C |
| 20 | call_externfunc | 1.061% | 52.31% | C | 92 | mulsd_regxmm_regxmm | 0.128% | 78.79% | |
| 21 | mov_reg4_dispstr | 1.046% | 53.36% | M | 93 | movabs_reg8_immval | 0.127% | 78.92% | M |
| 22 | test_reg4_reg4 | 0.936% | 54.30% | | 94 | mov_dwordptr[reg8+disp]_immval | 0.126% | 79.04% | M |
| 23 | push_bp8 | 0.891% | 55.19% | | 95 | shr_reg8_immval | 0.126% | 79.17% | |
| 24 | mov_reg4_dwordptr[bp8-disp] | 0.872% | 56.06% | M | 96 | movzx_reg4_byteptr[reg8] | 0.126% | 79.30% | M |
| 25 | sub_sp8_immval | 0.812% | 56.87% | | 97 | mov_bp4_immval | 0.124% | 79.42% | M |
| 26 | mov_qwordptr[sp8+disp]_reg8 | 0.808% | 57.68% | M | 98 | sar_reg8_immval | 0.123% | 79.54% | |
| 27 | mov_reg8_qwordptr[bp8-8] | 0.801% | 58.48% | M | 99 | cmp_reg2_immval | 0.117% | 79.66% | |
| 28 | add_sp8_immval | 0.786% | 59.26% | | 100 | jl_jmpdst | 0.116% | 79.78% | J |
| 29 | pop_bp8 | 0.757% | 60.02% | | 101 | lea_reg8_[reg8+reg8] | 0.115% | 79.89% | |
| 30 | mov_reg8_qwordptr[ip8+disp] | 0.690% | 60.71% | M | 102 | sub_reg4_reg4 | 0.114% | 80.01% | |
| 31 | lea_reg8_[bp8-disp] | 0.680% | 61.39% | | 103 | mov_reg1_immval | 0.113% | 80.12% | M |
| 32 | mov_reg8_qwordptr[reg8+8] | 0.680% | 62.07% | M | 104 | mov_reg8_qwordptr[disp] | 0.112% | 80.23% | M |
| 33 | lea_reg8_[sp8+disp] | 0.651% | 62.72% | | 105 | cmp_qwordptr[reg8+disp]_immval | 0.112% | 80.34% | |
| 34 | mov_reg8_bp8 | 0.622% | 63.35% | M | 106 | cmp_dwordptr[ip8+disp]_immval | 0.111% | 80.45% | |
| 35 | cmp_reg8_reg8 | 0.619% | 63.96% | | 107 | vmulsd_regxmm_regxmm_regxmm | 0.109% | 80.56% | |
| 36 | mov_reg4_dwordptr[reg8+disp] | 0.610% | 64.57% | M | 108 | lea_reg8_[reg8+reg8*8] | 0.107% | 80.67% | |
| 37 | mov_dwordptr[bp8-disp]_reg4 | 0.584% | 65.16% | M | 109 | mov_dwordptr[sp8+disp]_immval | 0.106% | 80.78% | M |
| 38 | mov_bp8_sp8 | 0.569% | 65.73% | M | 110 | movabs_reg8_dispstr | 0.106% | 80.88% | M |
| 39 | add_reg8_reg8 | 0.550% | 66.28% | | 111 | sete_reg1 | 0.105% | 80.99% | |
| 40 | mov_qwordptr[reg8+disp]_reg8 | 0.512% | 66.79% | M | 112 | jge_jmpdst | 0.103% | 81.09% | J |
| 41 | mov_reg4_dispdata | 0.470% | 67.26% | M | 113 | cmp_byteptr[reg8+disp]_immval | 0.101% | 81.19% | |
| 42 | and_reg4_immval | 0.466% | 67.73% | | 114 | js_jmpdst | 0.100% | 81.29% | J |
| 43 | mov_qwordptr[bp8-8]_reg8 | 0.459% | 68.19% | M | 115 | mov_dwordptr[reg8]_reg4 | 0.100% | 81.39% | M |
| 44 | test_reg1_reg1 | 0.426% | 68.61% | | 116 | sub_reg8_immval | 0.099% | 81.49% | |
| 45 | shl_reg8_immval | 0.422% | 69.03% | | 117 | shl_reg4_immval | 0.099% | 81.59% | |
| 46 | add_reg4_immval | 0.397% | 69.43% | | 118 | test_byteptr[reg8+disp]_immval | 0.096% | 81.68% | |
| 47 | lea_reg8_[reg8+disp] | 0.349% | 69.78% | | 119 | movapd_regxmm_regxmm | 0.096% | 81.78% | M |
| 48 | movsxd_reg8_reg4 | 0.332% | 70.11% | M | 120 | mov_qwordptr[sp8]_reg8 | 0.093% | 81.87% | M |
| 49 | mov_bp8_reg8 | 0.325% | 70.44% | M | 121 | mov_byteptr[bp8-disp]_reg1 | 0.093% | 81.97% | M |
| 50 | mov_reg4_dwordptr[sp8+disp] | 0.322% | 70.76% | M | 122 | mov_reg8_qwordptrfs:[disp] | 0.093% | 82.06% | M |
| 51 | mov_qwordptr[reg8]_reg8 | 0.299% | 71.06% | M | 123 | xor_reg8_qwordptrfs:[disp] | 0.093% | 82.15% | |
| 52 | mov_reg4_dwordptr[reg8] | 0.284% | 71.34% | M | 124 | cmp_dwordptr[reg8+disp]_immval | 0.093% | 82.24% | |
| 53 | call_qwordptr[reg8+disp] | 0.280% | 71.62% | C | 125 | push_immval | 0.092% | 82.34% | |
| 54 | ja_jmpdst | 0.278% | 71.90% | J | 126 | movsxd_reg8_dwordptr[bp8-disp] | 0.091% | 82.43% | M |
| 55 | mov_reg4_dwordptr[ip8+disp] | 0.262% | 72.16% | M | 127 | setne_reg1 | 0.091% | 82.52% | |
| 56 | cmp_reg4_reg4 | 0.245% | 72.41% | | 128 | mov_reg4_dwordptr[reg8+8] | 0.091% | 82.61% | M |
| 57 | jae_jmpdst | 0.240% | 72.65% | J | 129 | test_bp8_bp8 | 0.091% | 82.70% | |
| 58 | jle_jmpdst | 0.239% | 72.89% | J | 130 | lea_reg8_[reg8+reg8*2] | 0.090% | 82.79% | |
| 59 | sub_reg8_reg8 | 0.238% | 73.12% | | 131 | lea_reg8_[reg8+1] | 0.088% | 82.88% | |
| 60 | cmp_reg8_immval | 0.236% | 73.36% | | 132 | movzx_reg4_reg2 | 0.086% | 82.96% | M |
| 61 | jbe_jmpdst | 0.232% | 73.59% | J | 133 | lea_reg4_[reg8+1] | 0.086% | 83.05% | |
| 62 | mov_dwordptr[sp8+disp]_reg4 | 0.230% | 73.82% | M | 134 | mov_qwordptr[reg8]_dispdata | 0.086% | 83.13% | M |
| 63 | mov_qwordptr[reg8+disp]_immval | 0.227% | 74.05% | M | 135 | mov_bp4_reg4 | 0.084% | 83.22% | M |
| 64 | mov_reg8_qwordptr[bp8+disp] | 0.225% | 74.27% | M | 136 | vmovsd_regxmm_qwordptr[sp8+disp] | 0.084% | 83.30% | |
| 65 | mov_reg8_qwordptr[sp8+8] | 0.224% | 74.50% | M | 137 | addsd_regxmm_regxmm | 0.083% | 83.38% | |
| 66 | movzx_reg4_reg1 | 0.216% | 74.71% | M | 138 | mov_qwordptr[bp8-disp]_immval | 0.082% | 83.47% | M |
| 67 | add_reg4_reg4 | 0.211% | 74.92% | | 139 | vmovsd_qwordptr[sp8+disp]_regxmm | 0.081% | 83.55% | |
| 68 | jb_jmpdst | 0.211% | 75.14% | J | 140 | and_reg1_immval | 0.080% | 83.63% | |
| 69 | mov_dwordptr[reg8+disp]_reg4 | 0.195% | 75.33% | M | 141 | mov_reg8_qwordptr[bp8] | 0.080% | 83.71% | M |
| 70 | cmp_reg1_immval | 0.193% | 75.52% | | 142 | pxor_regxmm_regxmm | 0.080% | 83.79% | |
| 71 | leave | 0.186% | 75.71% | C | 143 | lea_reg8_[reg8+8] | 0.079% | 83.87% | |
| 72 | movzx_reg4_byteptr[reg8+disp] | 0.167% | 75.88% | M | 144 | mov_byteptr[reg8+disp]_immval | 0.078% | 83.94% | M |

Table 10: Top 144 normalized instructions and their frequencies in our dataset. The last 14% of total instructions has rarely seen with a long tail of the distribution (Figure 3). The group field indicates (C)all, (J)ump and (M)ove instructions.